ELSEVIER

Thermochimica Acta 304/305 (1997) 209–218

thermochimica acta

Evaluation of temperature-modulated differential scanning calorimetric measurements by phase-sensitive rectification techniques

G.W.H. Höhne*

Universität Ulm, Sektion für Kalorimetrie, D-89069 Ulm, Germany

Received 4 October 1996; accepted 14 March 1997

Abstract

The phase-sensitive rectification method (lock-in technique) is presented and tested to serve as another evaluation method for temperature-modulated differential scanning calorimetric measurements. This is done by model calculations with a mathematical computation system, using simple models of events often measured in this type of calorimeter: changes in heat capacity, cold crystallization, a chemical reaction and the glass transition. The advantages of the new evaluation method are: a lower numerical expenditure; a well-defined connection between time resolution and smoothing interval; and a reliable decrease in fluctuations of the results. It has furthermore been demonstrated that numerical calculations can be a powerful tool to test different models and their influence on the measured signal and the evaluated results. This is especially significant in cases, where a certain process produces non-linear distortions of the heat-flow rate signal. © 1997 Elsevier Science B.V.

Keywords: Cold crystallization; Glass transition; Model calculations; Reaction; Temperature-modulated differential scanning calorimetry (TM-DSC)

1. Introduction

Temperature-modulated measuring techniques has been introduced in differential scanning calorimetry (DSC) by Reading et al. [1]. There are several adequate commercial apparatus available from different manufactures. The respective numerical evaluation methods, which often are not known in detail, yield different results, for example 'reversing' and 'non-reversing' heat flow, or 'storage' and 'loss' heat capacity. Usually, the evaluation of the heat-flow rate function measured in commercial temperature-modulated DSC (TM-DSC) is carried out by a Fourier analysis method [2].

This method, which may be related to the attributes of complex numbers as well, yields at last the magnitude (absolute value, amplitude) and the phase of the heat-flow rate as a function of time. These quantities constitute the basis of further calculations.

Another evaluation method, often used to get information from a signal with known frequency, especially in presence of high noise levels, is the so-called phase-sensitive rectification (PSR) techniques. This technique is used in lock-in amplifiers which are able to separate periodic signals from a non-periodic (or periodic, but with other frequencies) background (noise) which may have an up-to-three orders of magnitude higher intensity.

The aim of this paper is to introduce this method, somewhat modified, in TM-DSC evaluation, test its

*Corresponding author.

PII S0040-6031(97)00182-2

usefulness by evaluation of some simulated measurements of typical thermal events inside the sample and compare it with the common evaluation method. The influence of heat transport processes on measurements is neglected here. This is done in order to better see the connection between different common processes inside the sample and the evaluated results. This may be helpful for discussion of real measurements from real DSC and the evaluation method in question.

2. Evaluation methods

In TM-DSC, the temperature–time function is

$$T(t) = T_0 + \beta t + T_a \sin(\omega t) \tag{1}$$

here, T_0 is the initial temperature, t the time, β the heating rate, $\omega = 2\pi/p$ the angular frequency, and p the period.

The corresponding heat-flow rate function $\Phi(t)$, in the ideal case (no delay), then reads:

$$\Phi(t) = \Phi_u(t) + \Phi_a \cos(\omega t) \tag{2}$$

In a real DSC, there is always a delay between the temperature change and the resulting heat flow caused by the limited heat transport leading to a phase shift δ_{th}. In addition, there may be another delay (and thus phase shift δ_p) of the signal caused by time-consuming processes in the sample which does not react immediately on temperature changes. Instead of Eq. (2), we now have to write:

$$\Phi(t) = \Phi_u(t) + \Phi_a \cos(\omega t - \delta) \tag{3}$$

with $\delta = \delta_{th} + \delta_p$ (The sign of δ follows from causality, the heat flow, which is the consequence, can only be after the cause, namely the temperature change.)

Both the temperature function (1) and the corresponding heat-flow rate (3) usually have a non-periodic ('underlying', Φ_u) and a periodic ($\tilde{\Phi}$) part. The former can be determined by 'gliding average' procedures, namely the summation from $t - p/2$ to $t + p/2$ and division by the respective number of values. The periodic part is calculated by subtracting the underlying part from the total one. The characteristic quantities of TM-DSC are usually determined from the periodic part, so we confine ourselves in the following to the evaluation of this function.

2.1. The common evaluation procedure

The method, used in commercial TM-DSC up to now, proceeds from the periodic part of the heat-flow rate function $\tilde{\Phi}(t)$ which is multiplied by $\sin(\omega t)$ and $\cos(\omega t)$, respectively, and integrated (gliding average) over one period:

$$\langle \tilde{\Phi}_{\sin}(t) \rangle \equiv \frac{2}{\omega} \int_{t-p/2}^{t+p/2} \tilde{\Phi}(t') \sin(\omega t') dt' = \Phi_a \sin\delta \tag{4}$$

$$\langle \tilde{\Phi}_{\cos}(t) \rangle \equiv \frac{2}{\omega} \int_{t-p/2}^{t+p/2} \tilde{\Phi}(t') \cos(\omega t') dt' = \Phi_a \cos\delta \tag{5}$$

From Eqs. (4) and (5), the amplitude and phase shift of the heat-flow signal can be calculated

$$\Phi_a(t) = \sqrt{\langle \tilde{\Phi}_{\sin}(t) \rangle^2 + \langle \tilde{\Phi}_{\cos}(t) \rangle^2} \tag{6}$$

$$\delta(t) = \arctan\left(\langle \tilde{\Phi}_{\sin}(t) \rangle / \langle \tilde{\Phi}_{\cos}(t) \rangle \right) \tag{7}$$

The amplitude $\Phi_a(t)$ contains information about the (static) heat capacity $C_p(t)$ of the sample and possibly additional information from temperature-dependent processes in the sample. From it (with the temperature amplitude T_a, the frequency ω and the (underlying) heating rate β) the 'reversing' component of the heat-flow rate is determined [1,3]:

$$\Phi_{rev}(t) = \Phi_u(t) - \Phi_{rev}(t) \tag{8}$$

The 'non-reversing' component is the difference between it and the underlying signal:

$$\Phi_{non}(t) = \Phi_u(t) - \Phi_{rev}(t) \tag{9}$$

The quantity $\delta(t)$ (Eq. (7)) contains both the phase shift related to the heat transport phenomena and that caused by time-consuming processes inside the sample. The former part is usually removed by suitable 'calibration' procedures, so the final output is usually $\delta_{sample}(t)$. However, a more sophisticated evaluation method [4] uses both the amplitude and phase information to calculate the complex heat capacity, where the real and imaginary part are the 'storage' and 'loss' heat capacities, respectively.

In every case, equations like Eqs. (4) and (5) and, thus, the gliding average procedure, are used to evaluate the measured signal. This method is easy and well-established from the mathematical point of view; nevertheless, the presuppositions for the exactness of it – a constant amplitude and phase during at least one period – are often not fulfilled. This results in periodical fluctuations of the average functions (see Section 3.1). To suppress these troubling fluctuations, often another smoothing of the data is done, but every smoothing results in a decrease of the resolution in time, faster processes in the sample are falsified and the output of the measurement is then only a 'smeared' picture of the truth.

2.2. The PSR method

The techniques used in lock-in amplifiers to get the amplitude of the periodic signal with a known frequency is the following:

The (pre-amplified) input signal is left as it is during the first half period of the reference signal (with the frequency in question) and inverted during the second half period (rectification) and then integrated over a selected time period Δt. Choosing Δt large (compared with the period of the signal of interest) the output signal is the average of the (positive) period of that signal that has the same frequency as the reference signal (Fig. 1, left side). No other component of the input signal contributes to the output. The reason is that the respective part of the rectified signal before integration oscillates around zero with a period (beat) equal to the difference of its frequency and the reference frequency, and consequently – if the integration period is large enough – its average value is zero (Fig. 1, right side).

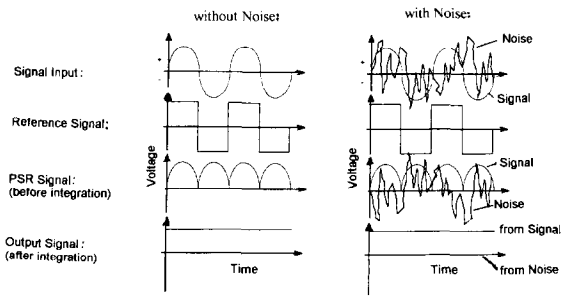

Fig. 1. Scheme of the phase-sensitive rectification (lock-in) technique for a signal which is in phase with the reference, in case of a 'pure' as well as a 'noisy' signal.

The connection between the integration period Δt and the frequency range $\Delta\nu$ (around the reference frequency), which contributes to the output signal of a lock-in amplifier, reads [see any textbook on electronics] as follows:

$$\Delta t \Delta \nu \approx 1 \tag{10}$$

Contributions of frequencies other than the reference frequency (but within the range $\Delta\nu$) are visible as oscillations of the output signal with a beat frequency equal to the frequency difference.

Applying this PSR method to TM-DSC evaluation requires some modifications. Normally the output signal, the heat-flow rate, is not in phase with the temperature oscillations, which otherwise easily could be used as reference signal. Nevertheless, the PSR method is practicable and the amplitude and phase shift of the periodic part follow from the results.

The periodic part of the heat-flow signal reads (cf. Eq. (3)):

$$\tilde{\Phi}(t) = \Phi_a \cos(\omega t - \delta) \tag{11}$$

If we assume that both the amplitude Φ_a and the phase shift δ are constant within the integration interval, which is chosen to be $p/2$, we get

$$I_1\left((2n-1)\frac{p}{4}\right) \equiv \int_{(n-1)p/2}^{np/2} \tilde{\Phi}(t)dt = \frac{2\Phi_a}{\omega}\sin\delta \quad (n = 1,3,5,\ldots) \tag{12a}$$

$$I_2\left((2n-1)\frac{p}{4}\right) \equiv \int_{(n-1)p/2}^{np/2} \tilde{\Phi}(t)dt = -\frac{2\Phi_a}{\omega}\sin\delta \quad (n = 2,4,6,\ldots) \tag{12b}$$

$$I_A\left(2n\frac{p}{4}\right) \equiv \int_{(2n-1)p/4}^{(2n+1)p/4} \tilde{\Phi}(t)dt = -\frac{2\Phi_a}{\omega}\cos\delta \quad (n = 1,3,5,\ldots) \tag{12c}$$

$$I_B\left(2n\frac{p}{4}\right) \equiv \int_{(2n-1)p/4}^{(2n+1)p/4} \tilde{\Phi}(t)dt = \frac{2\Phi_a}{\omega}\cos\delta \quad (n = 2,4,6,\ldots)$$

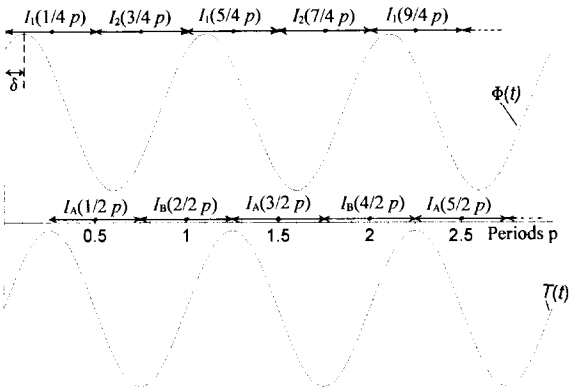

Fig. 2. Temperature ($T(t)$) and heat-flow rate ($\Phi(t)$) signal together with the two series of integration intervals for the PSR evaluation.

This looks complicated; however, it is not: there are two series of n integration intervals (marked with numbers and letters, respectively) (see Fig. 2), which are shifted towards one another by half an integration interval. Within these series, we get the same value of the integral apart from the alternating sign (which is indicated by different subscripts), as should be in this techniques. The abscissa was selected as the midpoint of the respective integration interval. To come to the same abscissa for both series, the mean value of two neighboring integrals of, e.g. the first series must be calculated first (cf. Fig. 2):

$$I_{12}\left(n\frac{p}{2}\right)=\frac{1}{2}\left(I_1\left((2n-1)\frac{p}{4}\right)-I_2\left((2n+1)\frac{p}{4}\right)\right) \quad (n=1,3,5,\ldots) \tag{13a}$$

$$I_{21}\left(n\frac{p}{2}\right)=\frac{1}{2}\left(I_1\left((2n-1)\frac{p}{4}\right)-I_1\left((2n+1)\frac{p}{4}\right)\right) \quad (n=2,4,6,\ldots) \tag{13b}$$

Again, both these mean integrals differ only in sign. From these results the desired quantities, amplitude and phase shift at the respective abscissa values can easily be calculated:

$$\Phi_a\left(n\frac{p}{2}\right)=\frac{\omega}{2}\left|\sqrt{I_{12}^2+I_A^2}\right| \quad \text{or} \quad =\frac{\omega}{2}\left|\sqrt{I_{21}^2+I_B^2}\right| \tag{14}$$

$$\delta\left(n\frac{p}{2}\right)=\arctan\left(-\frac{I_{12}}{I_A}\right) \quad \text{or} \quad =\arctan\left(-\frac{I_{21}}{I_B}\right) \tag{15}$$

We get one value of amplitude and phase shift, respectively, per integration interval and, consequently, two per period in this case (see, e.g. Fig. 4). The integration interval can even be chosen wider by calculating the proper average value from the integrals (Eqs. (12a),(12b),(12c) and (12d)). Further calculations have shown that from higher harmonics, (2ω, 3ω, ...) only the odd ones contribute to the above integrals and thus to amplitude and phase shift.

3. Model calculations of different thermal events

To test the reliability of the evaluation method, it is more useful to start from 'synthetic' measured curves obtained from numerical calculations for different well-known events rather than from real measurements, which often contain unknown influences from the apparatus. In a second step, the test with real measurements of known systems may be carried out.

For our calculations, we chose measurement parameters normally used in real TM-DSC, that is to say a heating rate of 0.5 to 2 K min^{-1}, a modulation period of 50 to 60 s, a modulation amplitude of 0.5 to 1.0 K, a sample heat capacity of 10 mJ K^{-1} and a data collection rate of 1 s^{-1}.

The expected heat-flow rate curve was calculated according to the theoretical model in question. All calculations were done with a mathematical computation system (MAPLE V Rel. 4, Waterloo Maple). The influence of heat-transport phenomena has not been taken into account, so only the influence from sample processes contribute to the results.

3.1. Influence of a non-constant heat capacity

In reality, the heat capacity is a weak function of temperature, inserting such a dependence into the heat-flow equation leads, however, to rather complicated integrals (cf. Eqs. (12a),(12b),(12c) and (12d)), which cannot be solved analytically. So we used, instead of the real temperature–time function (1), only the underlying part of it as a 0th approximation. This yields a linearly time-dependent heat capacity

$$C(T(t)) = C_0 + c_1 t \tag{16a}$$

and, with it, the following heat-flow rate function:

$$\Phi(t) = (C_0 + c_1 t)(\beta + \omega T_a \cos(\omega t - \delta)) \quad (16b)$$

The gliding average integral then reads in the 1st (linear) approximation:

$$\Phi_u \equiv \int_{t-p/2}^{t+p/2} \Phi(t')dt' = \beta p(C_0 + c_1 t) + c_1 p\left(\frac{\beta}{2}p + T_a \sin\delta\right) + 2c_1 T_a p\left(\cos\left(\frac{\omega}{2}t\right)\sin\left(\frac{\omega}{2}\right)\cos\delta - \cos^2\left(\frac{\omega}{2}t\right)\sin\delta\right) \quad (17)$$

This is again a sum of a non-periodic (underlying) and a periodic part. In the case of constant heat capacity ($c_1 = 0$), only the first augend on the right side remains, it is equal to the underlying heat-flow rate in Eq. (3). Otherwise a constant correction term appears and, in addition, a periodic part with period p and an amplitude proportional to the heat capacity change c_1. The respective results from both evaluation methods are shown in Figs. 3 and 4. The periodic fluctuations of Φ_u are clearly visible in both cases. With the common evaluation (Fig. 3), both Φ_a and δ fluctuate too, but with the double frequency. In the case of the PSR evaluation method, such fluctuations are not visible as there is only one value per fluctuation period which, however, is almost the same for both methods (see Figs. 3 and 4).

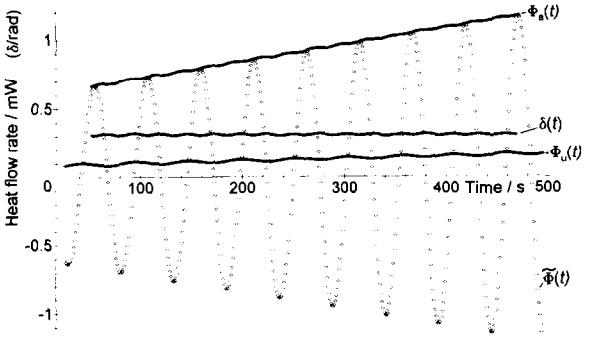

Fig. 3. Periodical ($\tilde{\Phi}(t)$) and underlying ($\Phi_u(t)$) heating rate, amplitude ($\Phi_a(t)$) and phase shift (δ) in the case of a time-(temperature)-dependent heat capacity, calculated with the common evaluation method.

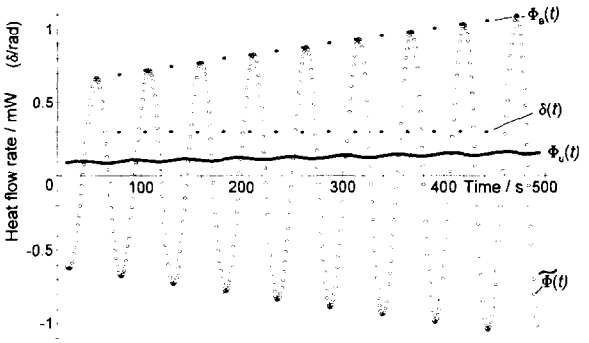

Fig. 4. Periodical ($\tilde{\Phi}(t)$) and underlying ($\Phi_u(t)$) heating rate, amplitude ($\Phi_a(t)$) and phase shift (δ) in the case of a time-(temperature)-dependent heat capacity, calculated with the PSR evaluation method.

3.2. *Influence of a non-constant phase shift*

A change of phase shift may appear by the changing heat-transfer conditions, or by certain other processes in the sample. Using the same procedure as explained in Section 3.1, with a linear approximation of the phase functions, sin δ and cos δ:

$$\delta(t) = \delta_0 + d_1 t \quad (18a)$$

$$\sin\delta(t) = \sin\delta_0 + d_1 t\cos\delta_0 \quad (18b)$$

$$\cos\delta(t) = \cos\delta_0 - d_1 t\sin\delta_0 \quad (18c)$$

the gliding average integral reads:

$$\Phi_u \equiv \int_{t-p/2}^{t+p/2} \Phi(t')dt' = \beta Cp + CpT_a d_1 \cos\delta_0 - 2CT_a p d_1\left(\cos\left(\frac{\omega}{2}t\right)\sin\left(\frac{\omega}{2}t\right)\sin\delta_0 + \cos^2\left(\frac{\omega}{2}t\right)\cos\delta_0\right) \quad (19)$$

The result is similar to that of Eq. (17), again we have a periodic component in addition to the expected underlying heat-flow rate function which, in addition, is modified by the second augend. The result in the case of common evaluation equals that of Fig. 3 in principle, again this fluctuation is clearly visible and both phase and amplitude fluctuate around the expected values. The respective result from PSR evaluation is given in Fig. 5.

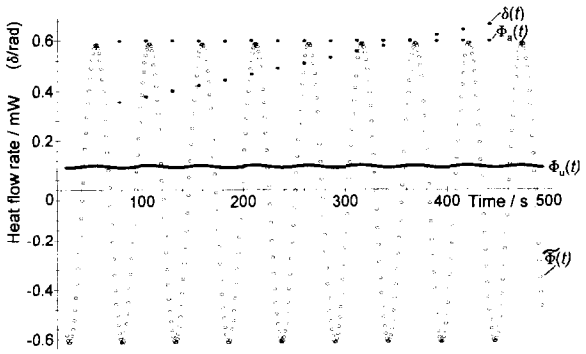

Fig. 5. Periodical ($\tilde{\Phi}(t)$) and underlying ($\Phi_u(t)$) heating rate, amplitude ($\Phi_a(t)$) and phase shift (δ) in the case of a time-(temperature-) dependent phase shift, calculated with the PSR evaluation method.

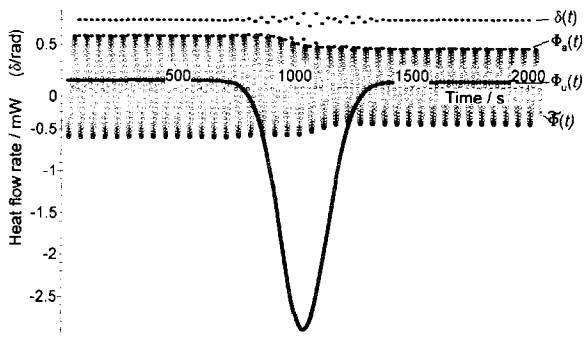

Fig. 6. Periodical ($\tilde{\Phi}(t)$) and underlying ($\Phi_u(t)$) heating rate, amplitude ($\Phi_a(t)$) and phase shift (δ) in the case of a 'cold crystallization', calculated with the PSR evaluation method.

3.3. The cold-crystallisation process

This process is well known from several glasses, which crystallize spontaneously some 10 K above the glass transition, often together with a heat-capacity change with the heat capacity of the solid being lower than that of the liquid state. Such a process is diffusion controlled and needs for that reason time, whereas small temperature changes do not influence the viscosity to any extent. That is why we simulated this event by a (Gauss-shaped) exothermic heat-flow rate function which is added to that from a heat capacity function which decreases in proportion to the degree of conversion from liquid to solid. The results are represented in Fig. 6. The amplitude and phase fluctuate in the region of the cold-crystallization as expected from the calculations of Sections 3.1 and 3.2, nevertheless the average values of the amplitude reflect the assumed heat capacity change while those of the phase change remain zero. This result is as expected for such a model.

3.4. Chemical reaction

For the sake of simplicity, we simulated a 1st-order elementary reaction which is described by the following Arrhenius-type equation:

$$\frac{dc}{dt} = -A\exp^{(-E_a/RT(t))}c(t) \qquad (20)$$

here, c is the concentration of reactant, A the pre-exponential factor, E_a the activation energy, R the gas constant, and T the temperature.

The change (decrease) of the reactant concentration depends on the temperature and on the present concentration, which changes in time. The heat production and, thus, the heat-flow rate from the sample is proportional to the concentration-change rate and thus a function of temperature and time. Solving the differential Eq. (20) of the 1st-order reaction in the case of time-dependent temperature gives:

$$\frac{dc}{dt}(t) = c_0 A\exp\left(-\int_0^t A\exp^{(-E_a/RT(t))}dt'\right) \times \exp^{(-E_a/RT(t))} \qquad (21)$$

The respective heat flow follows from the known initial concentration c_0 and from the total heat of reaction, which can easily be determined from the total heat-flow rate curve by integration.

The result of the calculation of such a reaction is represented in Figs. 7 and 8. As expected the influence of heat of reaction is only found in the underlying heat-flow rate, and the amplitude is constant apart from some fluctuations in the region, where the reaction heat-flow rate has a large curvature. The cause is similar to that of Section 3.1, but in this case Φ_u (instead of C) is changed during a period. Very unexpected, however, is the result of a non-zero phase shift in the reaction region. As the reaction rate in every moment is a function of the present temperature and concentration alone, there should not be any delay

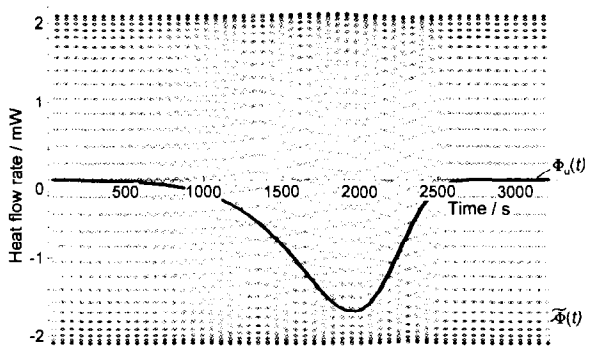

Fig. 7. Periodical ($\tilde{\Phi}(t)$) and underlying ($\Phi_u(t)$) heating rate in the case of a 1st-order reaction, calculated with the PSR evaluation method.

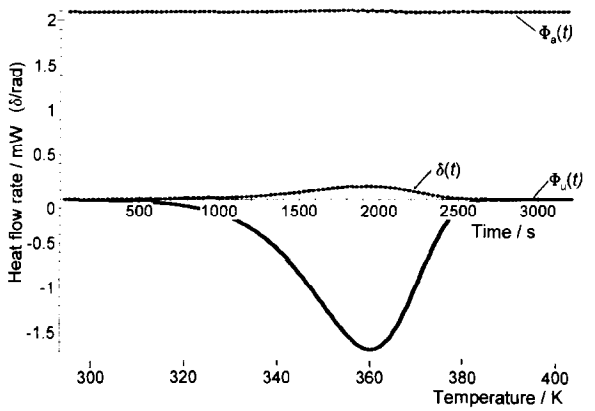

Fig. 8. Underlying ($\Phi_u(t)$) heating rate, amplitude ($\Phi_a(t)$) and phase shift (δ) in the case of a 1st-order reaction, calculated with the PSR evaluation method.

in heat production and, consequently, no phase shift between temperature and heat-flow rate signal. Nevertheless, a phase shift results from the calculation which can only be explained by non-linear distortion of the symmetric (sine-shaped) input signal to an asymmetric heat-flow rate output signal, caused by the continuous decrease of the concentration in time which in turn decreases the reaction rate during a temperature cycle. The asymmetric distortion of the output signal causes a phase shift which, in this case, would lead to wrong conclusions, if we were to calculate, say, a complex sample heat capacity from these results. The influence of non-linear distortions on the signal of a TM-DSC and on the evaluation results has to be investigated in detail in the future, because such distortions cannot be excluded in every day research with this apparatus and could lead to wrong conclusions.

3.5. The glass process

This process describes a transition of amorphous materials from a non-equilibrium solid state to an equilibrium liquid state. Several theoretical models to describe this process are known from the literature. We chose two rather different approaches to test our evaluation method, namely a description which starts from a complex heat-capacity function and another which proceeds from a differential equation. As these models are only used to investigate the influence on the results of our evaluation method, we desist from entering further into details of the background of the respective theories but simply apply them in the calculation.

3.5.1. The differential equation approach

One model starts from 'holes' which can be 'solved' in the amorphous material and make a contribution to the enthalpy of this amorphous material. The change of the number of holes with temperature implies a corresponding change of the enthalpy with temperature (i.e. a slope change) and thus a change of the heat capacity:

$$\Delta C_{\text{hole}} = E_{\text{hole}} \frac{dN}{dt} \tag{22}$$

The quantitative description of the hole model reads as follows [5]:

$$\frac{dN}{dt} = \frac{1}{\tau(t)} (N^*(t) - N(t)) \tag{23}$$

The rate of change of the number of holes is proportional to the difference between the equilibrium number N^* and the real number $N(t)$ at a certain moment. The reciprocal proportionality constant is the relaxation time τ. N^* is linearly, and τ exponentially dependent on temperature within the glass-transition region and the following is valid:

$$N^*(T) = N_0^* + n_1^* T \tag{24}$$

$$\tau(t) = \tau_0 \exp(E_a/RT) \tag{25}$$

here, n_1^* is the proportionality factor and E_a the activation energy)

Inserting Eqs. (24) and (25) into Eq. (23) results in a differential equation, where the change rate of N (and thus the heat capacity) is a rather complex function of time- and temperature-dependent quantities. Nevertheless, this equation can be solved numerically in the case of TM-DSC. This is done by starting at a certain moment at a temperature above the glass transition, where the number of holes is in equilibrium (Eq. (24)), and calculating its change at that temperature for one time step (Eq. (23)).

Afterwards, the number of holes in every following moment can be calculated by steps, and from Eqs. (23) and (22) the heat capacity in question or the respective heat-flow rate. The result of this calculation is shown in Figs. 9–12 for a cooling and subsequent heating run. Amplitude and phase shift changes as expected from theoretical and experimental knowledge. The small non-zero phase shift in the liquid region (at high temperatures) is an artefact, which is caused by the numerical, stepwise, calculations. In the heating run, the so-called 'overheating' or 'enthalpy-relaxation' peak is clearly visible.

The fluctuations of the underlying heat-flow rate in the transition region are distinctly larger than in the examples before, the reason being that both phase and heat capacity changes in this region together lead to an enhanced influence on Φ_u.

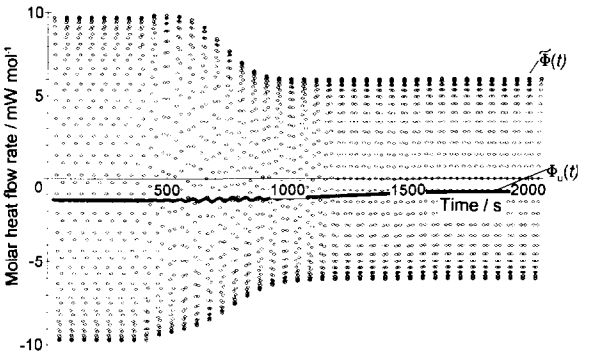

Fig. 9. Periodical ($\tilde{\Phi}(t)$) and underlying ($\Phi_u(t)$) heating rate in the case of a glass transition on cooling, calculated with the PSR evaluation method, using the 'hole model'.

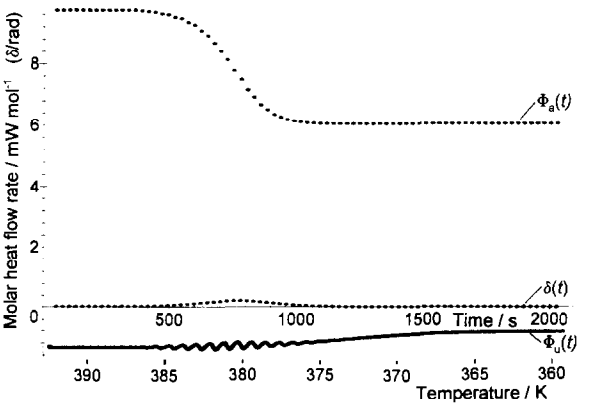

Fig. 10. Underlying ($\Phi_u(t)$) heating rate, amplitude ($\Phi_a(t)$) and phase shift (δ) in the case of a glass transition on cooling, calculated with the PSR evaluation method, using the 'hole model'.

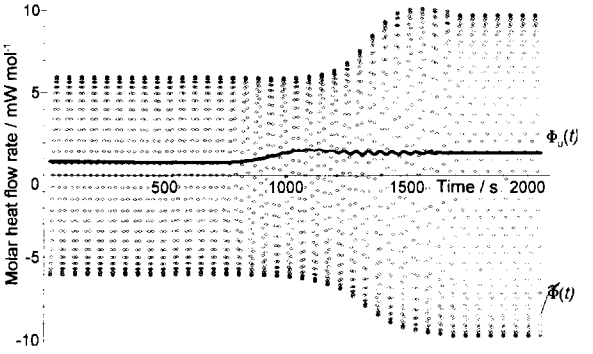

Fig. 11. Periodical ($\tilde{\Phi}(t)$) and underlying ($\Phi_u(t)$) heating rate in the case of a glass transition on heating, calculated with the PSR evaluation method, using the 'hole model'.

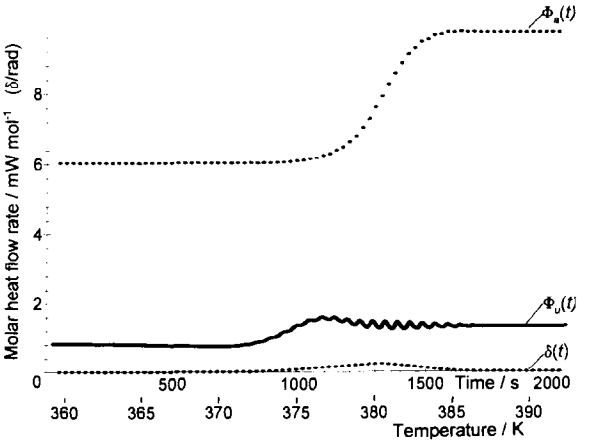

Fig. 12. Underlying ($\Phi_u(t)$) heating rate, amplitude ($\Phi_a(t)$) and phase shift (δ) in the case of a glass transition on heating, calculated with the PSR evaluation method using the 'hole model'.

3.5.2. The complex heat capacity approach

Another very simple model of the dynamic glass transition starts from a complex heat capacity in the ω-space with the following real (C') and imaginary (C'') parts [6]:

$$C'(\omega) = C_0 + \frac{\Delta C}{1 + (\omega\tau)^2} \tag{26a}$$

$$C''(\omega) = \frac{\Delta C \omega t}{1 + (\omega\tau)^2} \tag{26b}$$

where $\tau(T)$ is the same function as in Eq. (25). The corresponding heat-flow rate reads:

$$\Phi(t) = T_a\omega(C'\cos\omega\tau - C''\sin\omega\tau) \tag{27}$$

The respective calculation results are shown in Figs. 13 and 14, they contain the expected behaviour. The underlying heat-flow rate is almost zero, because of the definition (Eq. (27)) which does not contain that part of the heat-flow rate function which originates from the underlying heating rate, but only the dynamic part. Again, fluctuations in the underlying heat-flow rate function are visible in the region where the heat capacity and phase change.

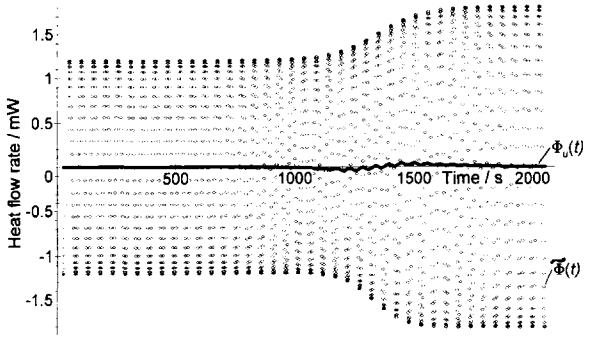

Fig. 13. Periodical ($\tilde{\Phi}(t)$) and underlying ($\Phi_u(t)$) heating rate in the case of a glass transition on heating, calculated with the PSR evaluation method, using a given complex heat capacity.

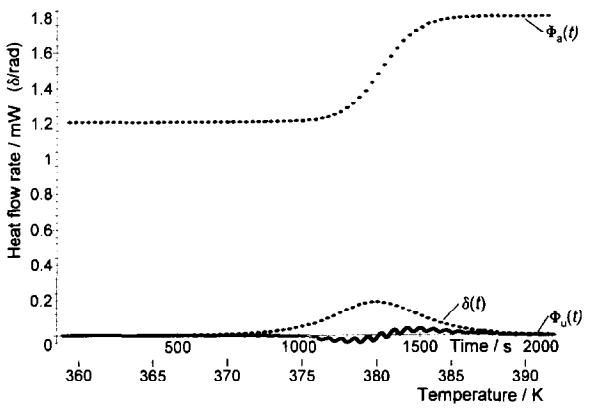

Fig. 14. Underlying ($\Phi_u(t)$) heating rate, amplitude ($\Phi_a(t)$) and phase shift (δ) in the case of a glass transition on heating, calculated with the PSR evaluation method using a given complex heat capacity. Evaluation of TM-DSC measurements by the phase-sensitive rectification technique.

4. Conclusions

The advantages of the PSR method are:

(i) There are only two values of amplitude and phase per period and the distance between them reflects the real resolution in time, whereas the gliding average method (Section 2.1) results in as many values as measuring points (usually 1...4 per second) which pretends a resolution in time (often $p/50$) far from the theoretical resolution which cannot be smaller than the integration interval (often p).

(ii) The smaller integration interval (at least in the 2nd set of integrals Eqs. (12a),(12b),(12c) and (12d) leads to a resolution ($\Delta t = p/2$) which is better than for the common method ($\Delta t = p$), nevertheless the corresponding band width (Eq. (10)) is $\Delta\nu \equiv 2/p = 2\nu$ (or $\Delta\omega = 2\omega$). This covers the frequency range from zero to 2ω, which is indeed broader than in the common case (where $\Delta\omega = \omega$); but, as the 2nd harmonic is totally suppressed in every case, this does not matter. The increase of noise (by a factor of two) usually does not matter as well.

(iii) The bandwidth can be reduced by choosing a larger (than $p/2$) integration time interval, to decrease the influence of non-linear distortions which produce a certain $\Delta\omega$-distribution around the frequency in question. Indeed the time resolution is decreased too, but the quantitative connection is well known from Eq. (10) and cannot lead to any false interpretation.

(iv) The fluctuations of Φ_a and δ, caused by changes of the heat capacity and the phase, respectively, are suppressed for the most part, because there is only one data point per fluctuation period (see Section 3.1) already representing the mean value of that interval, so an additional smoothing is not necessary.
(v) The numeric expense of evaluation is reduced considerably.

To sum up, there is indeed no need to change the common evaluation method, as it works correctly. However, the very large number of values, which this method yields, suggests a wrong information density and requires considerably more evaluation expense. The PRS method, on the other hand, comes to the same results faster and reflects immediately the proper time resolution. Choosing wider integration intervals (within the framework of the PSR techniques) suppresses possible non-linear distortions, but the experimenter is simultaneously informed about the price for it, namely the decreased time resolution which is visible in the lower number of values per time interval. He may then reflect whether he has chosen the proper frequency or/and underlying heating rate to investigate a certain process.

It has furthermore been demonstrated, that numerical calculations can be a powerful tool to test different models and their influence on the measured signal and the evaluated results. This is especially significant in cases, where a certain process produces non-linear distortions of the heat-flow rate signal.

Acknowledgements

The author thanks his colleagues from the 4th Lähnwitz Seminar and especially C. Schick and J.E.K. Schawe for helpful discussions.

References

[1] P.S. Gill, S.R. Sauerbrunn and M. Reading, J. Thermal Anal., 40 (1993) 931–939.
[2] B. Wunderlich, ATHAS report (1996).
[3] B. Wunderlich, Y. Jin and A. Boller, Thermochim. Acta, 238 (1994) 277–293.
[4] J.E.K. Schawe, Thermochim. Acta, 261 (1995) 183–194.
[5] L.C. Thomas, A. Boller, I. Okazaki and B. Wunderlich, Thermochim. Acta, 291 (1997) 85–94.
[6] J.E.K. Schawe, personal communication.